Proceedings of the 11th Brazilian Congress of Thermal Sciences and Engineering -- ENCIT 2006
Braz. Soc. of Mechanical Sciences and Engineering -- ABCM, Curitiba, Brazil,- Dec. 5-8, 2006

Paper CIT06-0308

EXPERIMENTAL THERMAL-HYDRAULIC ANALYSIS OF THE IPR-R1 TRIGA NUCLEAR REACTOR

Amir Zacarias Mesquita
Centro de Desenvolvimento da Tecnologia Nuclear – CDTN/CNEN
Campus da UFMG – Pampulha. CEP: 30.123-970 - Belo Horizonte/MG
amir@cdtn.br

Hugo César Rezende
Centro de Desenvolvimento da Tecnologia Nuclear – CDTN/CNEN
Campus da UFMG – Pampulha. CEP: 30.123-970 - Belo Horizonte/MG
hcr@cdtn.br

Abstract. *The heat generated by nuclear fission in the IPR-R1 nuclear reactor is transferred from fuel elements to the cooling system through the fuel/cladding (gap) and the cladding to coolant interfaces. The fuel thermal conductivity and the heat transfer coefficient from the cladding to the coolant were evaluated experimentally. A correlation for the gap conductance between the fuel and the cladding was also presented. As the reactor core power increases, the heat transfer regime from the fuel cladding to the coolant changes from single-phase natural convection to subcooled nucleate boiling. Results indicated that subcooled boiling occurs at the cladding surface in the reactor core central channels at power levels in excess of 60 kW.*

Keywords*. TRIGA Nuclear Reactor, heat transfer, subcooled boiling*

1. Introduction

The IPR-R1 TRIGA Nuclear Research Reactor, of the Nuclear Technology Development Center (CDTN), is a pool type reactor cooled by natural circulation and having as fuel an alloy of zirconium hydride and uranium enriched at 20% in ^{235}U. Figure (1) shows a photo of the reactor core and Fig. (2) shows a drawing of the reactor pool. The reactor has 59 aluminum-clad fuel elements and 5 stainless steel-clad fuel elements. One of these steel-clad fuel elements is instrumented with three chromel/alumel thermocouples along its center. Figure (3) shows the diagram and design of the instrumented fuel element (Gulf General Atomic, 1972). The fuel element data used in the calculations are found in the Table (1) (Mesquita, 2005).

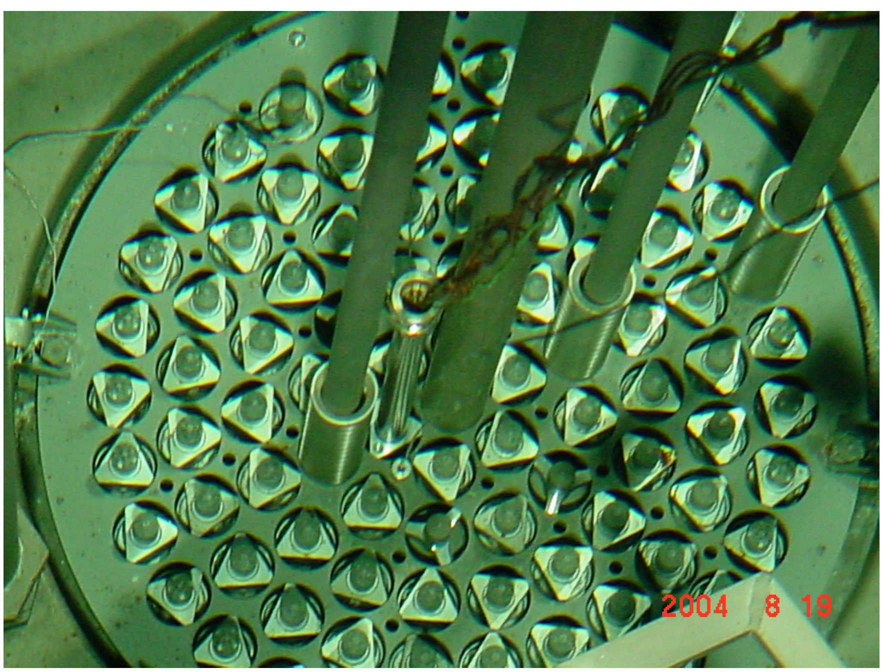

Figure 1. Core upper view with the instrumented fuel element in ring B.

The heat generated by fissions is transferred from fuel elements to the cooling system through a fuel/cladding interface (gap) and from the cladding to the coolant. The objective of the thermal and hydrodynamic projects of the reactors is to remove the heat safely, without producing excessive temperature in the fuels. The regions of the reactor core where boiling occurs can be determined from the heat transfer coefficient data at various power levels.

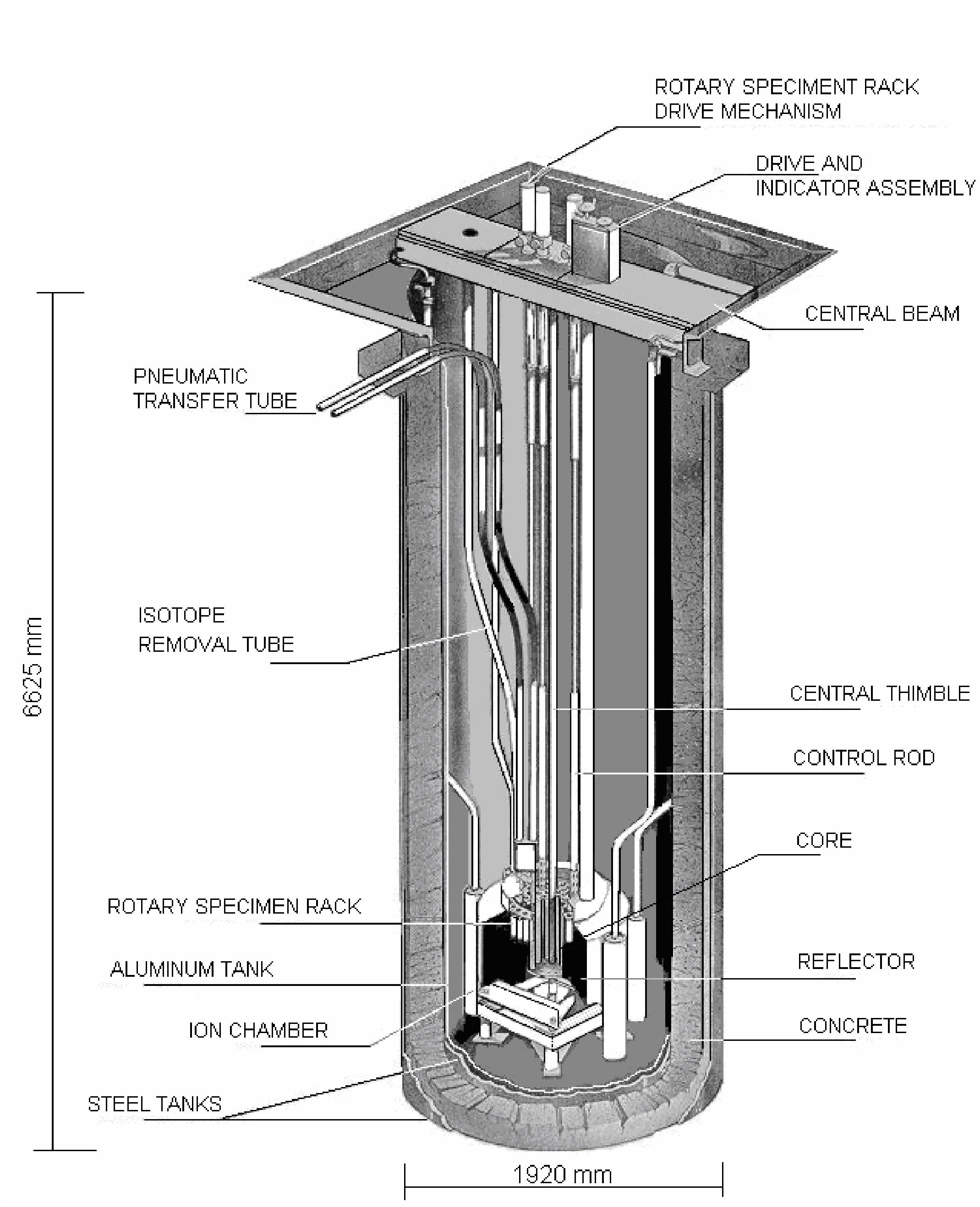

Figure 2: The TRIGA IPR-R1 Research Nuclear Reactor

The thermal conductivity (*k*) of the metallic alloys depends on several factors like temperature. In nuclear fuels, this is more complicated because *k* also becomes a function of irradiation as a result of change in the chemical and physical composition (porosity changes due to temperature and fission products). The major factors that affect the fuel thermal conductivity are temperature, porosity, oxygen to metal atom ratio, PuO_2 content, pellet cracking, and burnup. After the fuel alloy, the second largest resistance to heat conduction in the fuel rod is due to the gap. Several correlations exist (Todreas, 1990) to evaluate its value in power reactors fuels, which use mainly uranium oxide. The only reference found to TRIGA reactor's fuel is General Atomic (1970), that recommends the use of three hypotheses for the heat transfer coefficient in the gap. The heat transfer coefficient (*h*) is not only a property of the system but also depends on the fluid properties. The determination of *h* is a complex process that depends on the thermal conductivity, density, viscosity, velocity, dimensions and specific heat. All these parameters are temperature dependent and change while wall transfer heat to the fluid. An operational computer program and a data acquisition and signal processing system were developed as part of this research project (Mesquita, 2005) to allow on line monitoring of the operational parameters.

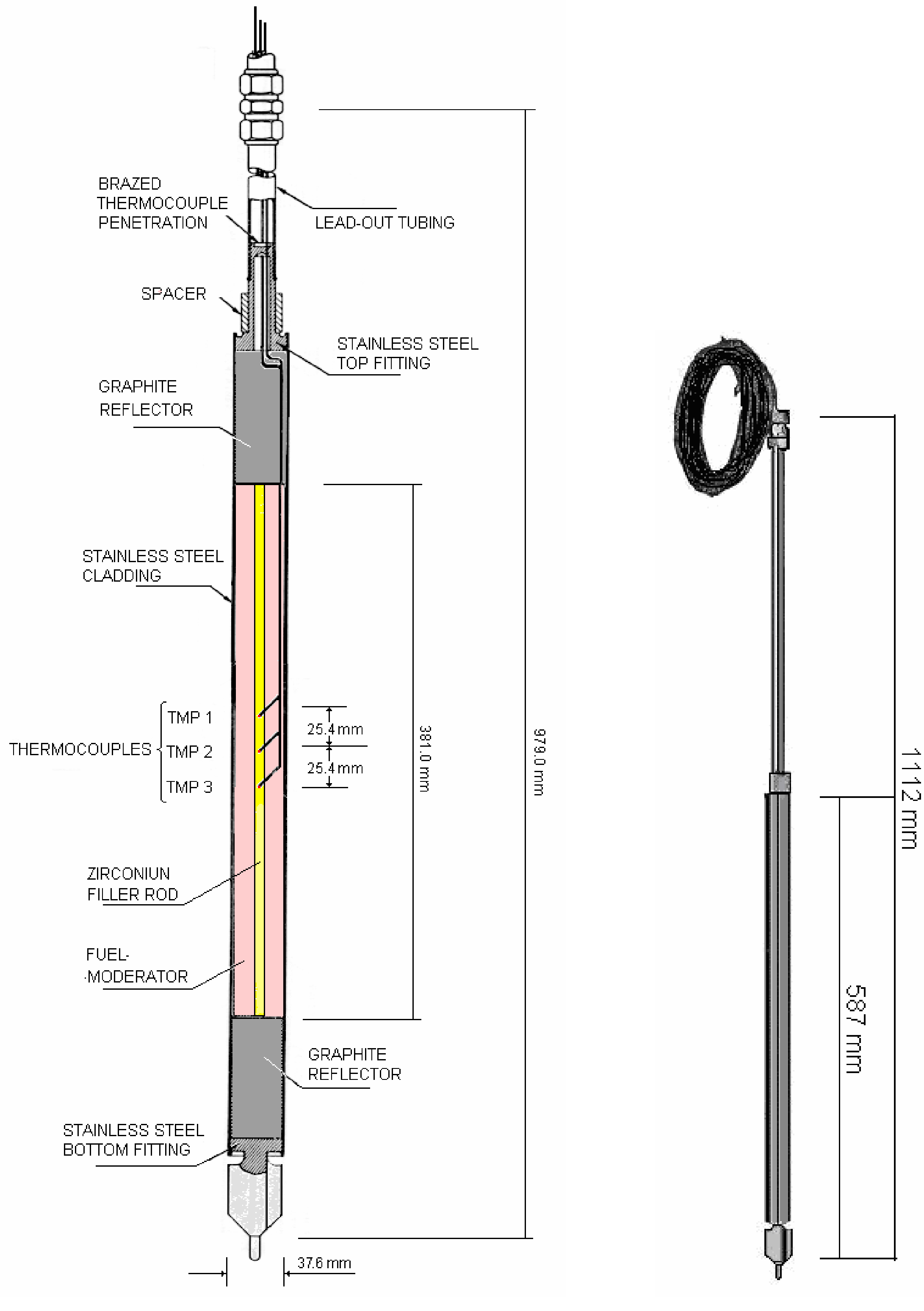

Figure 3. Instrumented fuel element.

Table 1. Instrumented fuel element data (Mesquita, 2005)

Parameter	Value
Heated length	38.1 cm
External diameter	3.76 cm
External fuel element active area	450.05 cm^2
External fuel area (U-$ZrH_{1.6}$)	434.49 cm^2
Fuel element active volume	423.05 cm^3
Fuel volume (U-$ZrH_{1.6}$)	394.30 cm^3
Power (total in the core = 265 kW)	4.518 kW

2. Overall thermal conductivity of the fuel elements

The expression below, for the overall thermal conductivity (k_g) for cylindrical fuel elements, in [W/mK], was obtained from Fourier equation (Lamarsh, 2001) (Duderstadt and Hamilton, 1976):

$$k_g = \frac{q''' r^2}{4(T_o - T_{sur})} \quad , \tag{1}$$

where, q''' is the volumetric rate of heat generation [W/m^3], T_o and T_{sur} are the central temperature and the fuel surface temperature [^oC] and r is the fuel element radius [m].

The temperature at the center of the fuel was measured. At the power of 265 kW, the heat transfer regime is the subcooled nucleate boiling in all of the fuel elements. The cladding outside temperature is the water saturation temperature (T_{sat}) at the pressure of 1.5 bar (atmospheric pressure added up of the water column of ~ 5.2 m), increased of the wall superheat (ΔT_{sat}). The superficial temperature (T_{sur}), in [^oC], is found by using the expression below, where T_{sat} is equal to 111.37 ^oC (Wagner and Kruse, 1998).

$$T_{sur} = T_{sat} + \Delta T_{sat} \quad . \tag{2}$$

The wall superheat is obtained by using the correlation proposed by McAdams (Tong and Weisman, 1996),

$$\Delta T_{sat} = 0.81(q'')^{0.259} , \tag{3}$$

with q'' in [W/m^2] and T_{sat} in [^oC].

A fuel element was introduced in position B1, which was instrumented with three type K thermocouples as shown in Fig. (1). Two thermocouples were also placed in two core channels the closest as possible to position B1.

3. Heat transfer in the reactor core

3.1. Single-phase region

The heat transfer coefficient in single-phase region (h_{sp}) was calculated with the Dittus-Boelter correlation (Glasstone and Sesonske, 2001), valid for turbulent flow in narrow channels, given for:

$$h_{sp} = 0.023 \frac{k}{D_w} \left(\frac{G D_w}{\mu} \right)^{0.8} \left(\frac{c_p \mu}{k} \right)^{0.4} , \tag{4}$$

where: $D_w = 4A/P_w$ is the hydraulic diameter of the channel based on the wet perimeter; A is the flow area [m^2]; P_w is the wet perimeter [m]; G is the mass flow [kg/m^2s]; c_p is the isobaric specific heat [J/kgK]; k is the thermal conductivity [W/mK]; and, μ is the fluid dynamic viscosity [kg/ms]. The fluid properties for the IPR-R1 TRIGA core are calculated for the sub-saturated bulk water temperature at 1.5 bar.

The two hottest channels in the core are the Channel 0 and the Channel 1', shown in Fig. (4). The heat transfer coefficient was estimated by using the Dittus-Boelter correlation. The inlet and outlet temperatures in Channel 0 were considered as being the same of Channel 1'. The geometric data of Channel 0 and Channel 1' and the percent contributions of each fuel to the heat power transferred to the water along the two channels are given in Table (2).

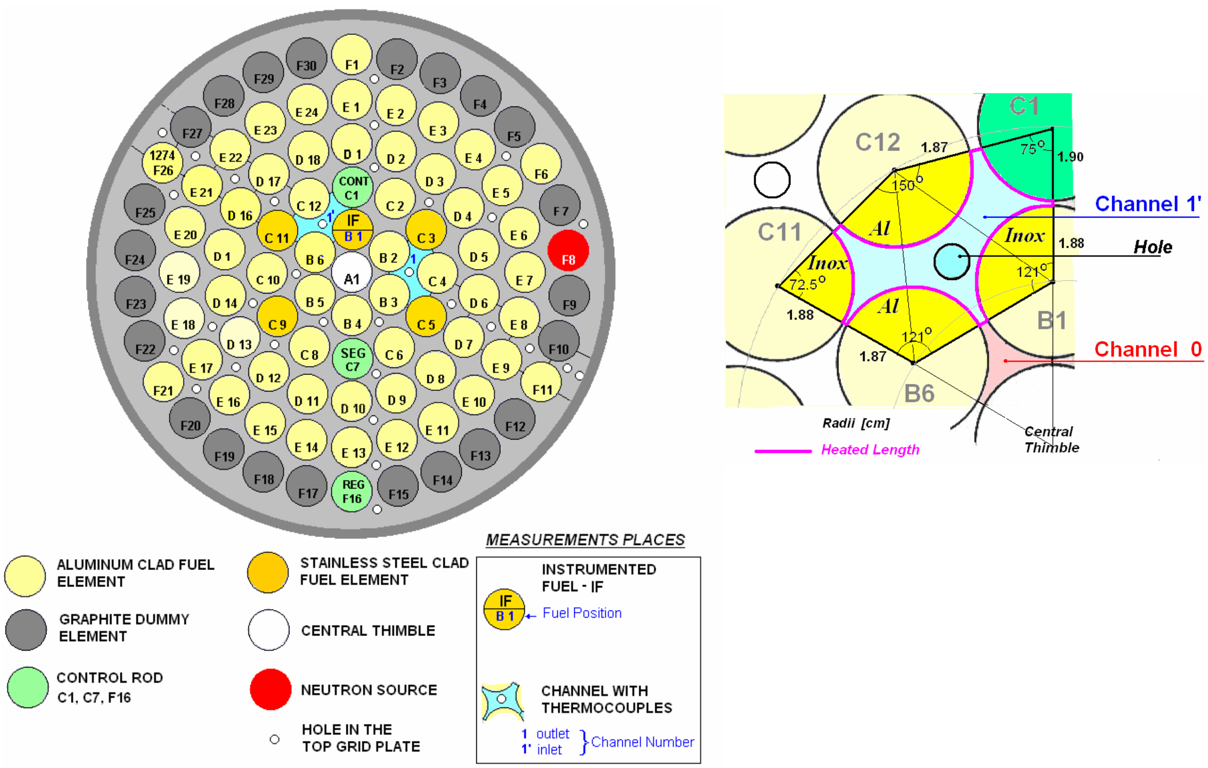

Figure 4. The IPR-R1 core configuration and the two hottest coolant channels.

Table 2. Channel 0 and Channel 1' characteristics (Mesquita, 2005).

	Channel 0	Channel 1'	Unit
Area (A)	1.574	8.214	cm^2
Wet perimeter (P_w)	5.901	17.643	cm
Heated Perimeter (P_h)	3.906	15.156	cm
Hydraulic diameter (D_w)	1.067	1.862	cm
B1 and C1 Fuel Diameter (inox)	3.76	3.76	cm
B6 and C12 Fuel Diameter (Al)	3.73	3.73	cm
C1 Control Rod Diameter	3.80	3.80	cm
Central Thimble Diameter	3.81	3,81	cm
Core Total Power (265 kW)	100	100	%
B1 Fuel Contribution	0.54	1.11	%
B6 Fuel Contribution	0.46	0.94	%
C11 Fuel Contribution	-	0.57	%
C12 Fuel Contribution	-	1.08	%
Total Power of the Channel	1.00	3.70	%

The mass flux is given indirectly from the thermal balance across the channel using measurements of the water inlet and outlet temperatures:

$$q = \dot{m} c_p \Delta T \,, \tag{5}$$

where: q is the power supplied to the channel [kW]; is the mass flow rate in the channel [kg/s]; c_p is the isobaric specific heat of the water [J/kgK]; and, ΔT is the temperature difference across the channel [^{o}C].

The reactor was operated on steps of about 50 kW until 265 kW and data were collected as function of the power supplied to Channel 1' and Channel 0. The water thermodynamic properties at a pressure of 1.5 bar were obtained from Wagner and Kruse (1998) as a function of the bulk water temperature in the channel. The curves of single-phase heat transfer are presented in the Fig. (5) as function of ΔT_{sat}. The curve for heat transfer coefficient (h_{sur}) in the single-phase region is shown in Fig. (6) as function of the power.

3.2. Subcooled nucleate boiling region

The expression used for the subcooled nucleate boiling region is shown below (Kreith and Bohn, 2001), (Tong and Tang, 1997):

$$h_{sur} = q'' / \Delta T_{sat} \,, \tag{6}$$

where: h_{sur} is the convective heat-transfer coefficient from the fuel cladding outer surface to the water [kW/m^{2}K]; q'' is the fuel surface heat flux [kW/m^2]; and, ΔT_{sat} is the surface superheat in contact with the water [^{o}C], given by McAdams correlation (Eq. 3).

Figure (5) presents the fuel element surface heat transfer coefficient for the coolant as a function of the superheat, in both regimes. This curve is specific for the fuel in position B1 at IPR-R1 TRIGA reactor conditions. The correlation used for subcooled nucleate boiling is not valid for single-phase convection region as well as the Dittus-Boelter correlation is not valid for the boiling region. The transition point between single-phase convection regime (Channel 1) to subcooled nucleate boiling regime (onset of nucleate boiling) is approximately 60 kW as shown in the graph by the two pink line intersection.

Figure (6) presents the curves for the heat transfer coefficient (h_{sur}) on the fuel element surface and for the overall thermal conductivity (k_g) in fuel element as function of the power, obtained for the instrumented fuel at B1 core position.

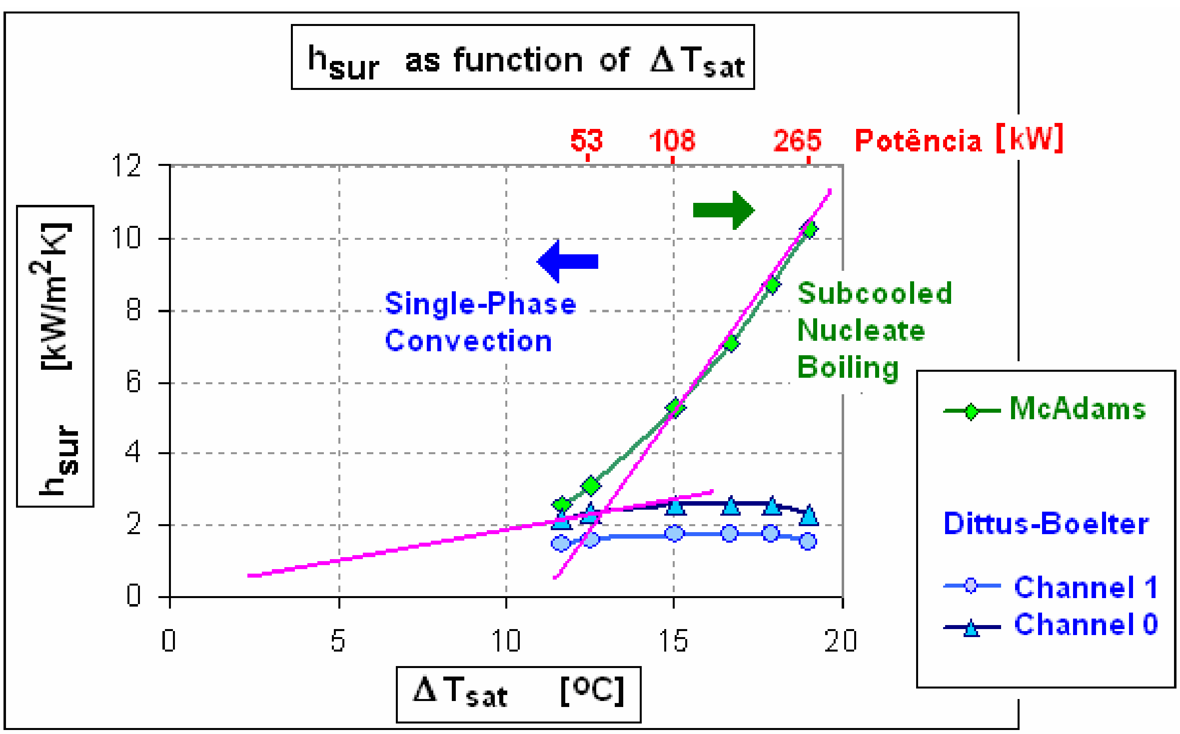

Figure 5. Heat-transfer regimes in the fuel element surface.

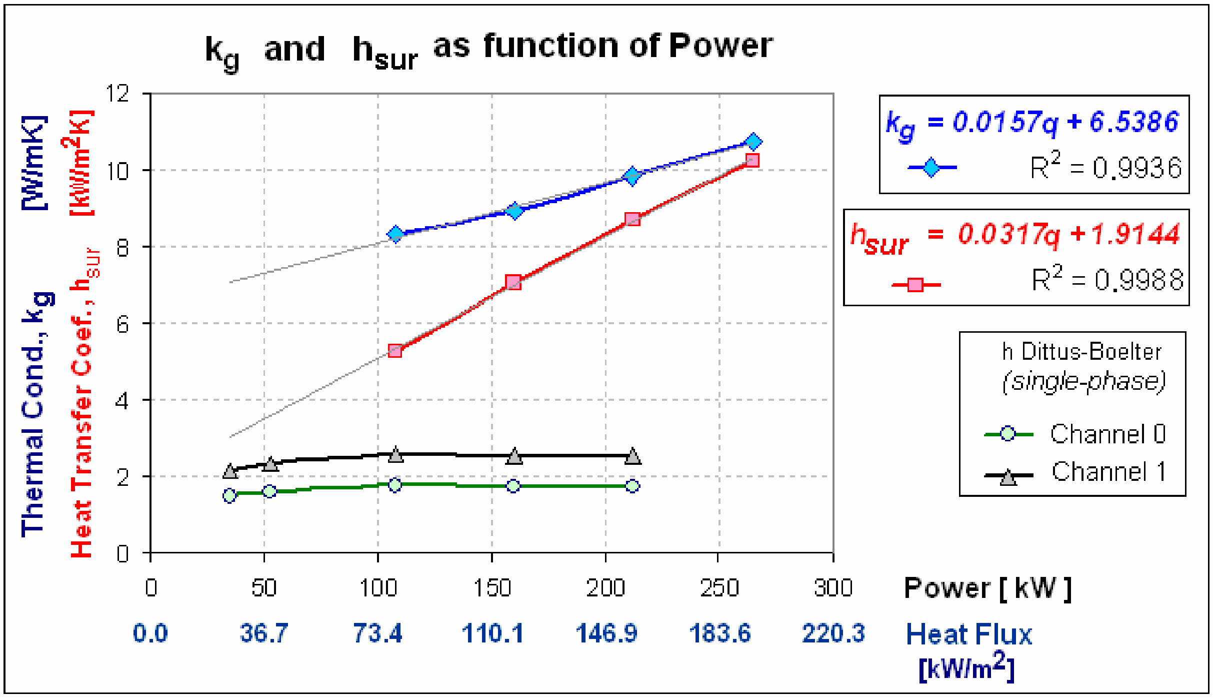

Figure 6. Overall fuel element thermal conductivity and cladding heat transfer coefficient to the coolant.

4. Heat transfer coefficient in the fuel gap

The instrumented fuel element is composed of a central zirconium filler rod with 6.25 mm in diameter, the active part of the fuel, which is formed by uranium zirconium hydride alloy (U-$ZrH_{1.6}$), an interface (gap) between the fuel and the cladding and, finally, the 304 stainless steel cladding. The thermocouples are fixed in the central rod. It is supposed that all heat flux is in the radial direction. Using the analogy with electric circuits, the resistance to the heat conduction from the fuel center to the coolant (R_g) is given by the sum of the resistances of the fuel components.

The fuel element configuration is shown in the Fig. (7). The axial heat conduction and the presence of the central pin of zirconium were not considered. The thermal conductivity (k_{rev}) equations for the fuel components, in [W/mK], are given in the Table (3) as function of temperature *(T)* in [^{o}C]. Three expressions for the uranium/zirconium alloy were found in the technical literature. It was used the equation of Simnad et al. (1976).

Table 3. Thermal conductivity as function of temperature

Material	*k (T)*	Reference
Zirconium (Zr)	4.0×10^{-3} T + 21.23	Glasstone and Sesonske (1994)
Uranium zirconium hydride (U-$ZrH_{1,6}$)	1.11×10^{-3} T + 18.5	General Atomic (1969)
	0.0075 T + 17.58	Simnad et al. (1976)
	0.00415 T + 18.94	Ahad et al. (1992)
Steel AISI 304	$3.17\text{x } 10^{-9}\text{x}T^3 - 6.67 \times 10^{-6}T^2 + 1.81 \text{ x}10^{-2}T + 14.46$	ASME (1992)

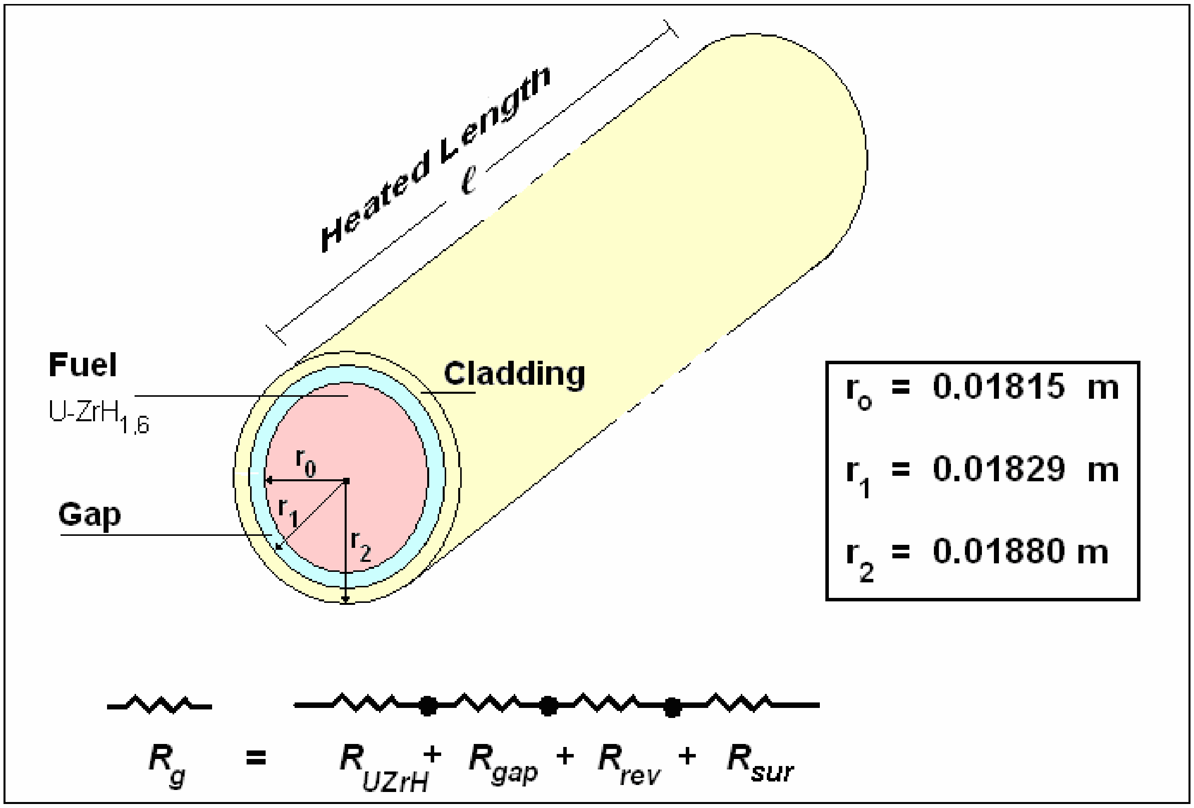

Figure 7. Fuel element configuration

The value of R_{gap} is the value of the overall resistance of the fuel element (R_g) less the values of the others components resistance. It was found from the values of k_g and h_{sur} obtained previously and from the values of k for the fuel alloy and for the cladding, both corrected in function of temperature. The heat transfer coefficient in the gap is:

$$h_{gap} = \frac{2}{r_0}\left(\frac{k_g k_{UZrH} k_{rev}}{k_{UZrH} k_{rev} - k_g k_{rev} - 2k_g k_{UZrH} \ell n(r_2 / r_1)} \right) \tag{7}$$

The graph of the heat transfer coefficient through the gap is shown in the Fig. (8) as a function of the reactor power. This figure also shows three theoretical values for the heat transfer coefficient recommended by General Atomic (1970).

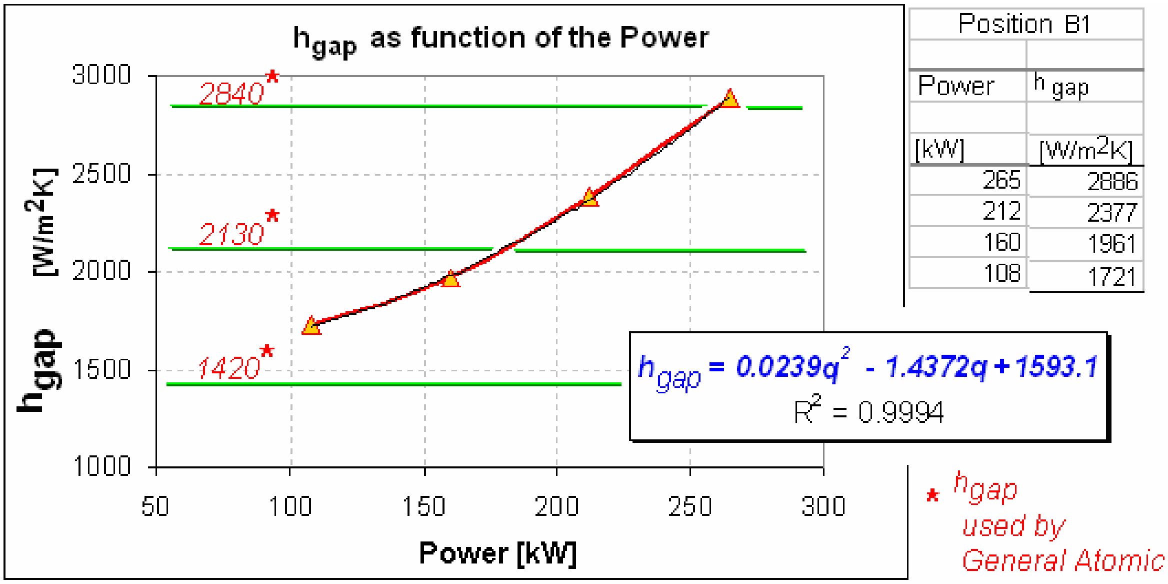

Figure 8. Heat transfer coefficient through the gap as a function of the power.

5. Fuel rod temperature profile

It is possible to obtain the radial temperature distribution in the fuel element from the temperature in the center of the fuel and using the conduction equations for the fuel element geometry. Figure (9) shows the experimental radial profile of maximum fuel temperature in position B1 and compares it with the results of PANTERA code (Veloso, 2005). The instrumented fuel element was used to measure the fuel temperature at many reactor powers. The results are shown in Fig. (10) and Table (4).

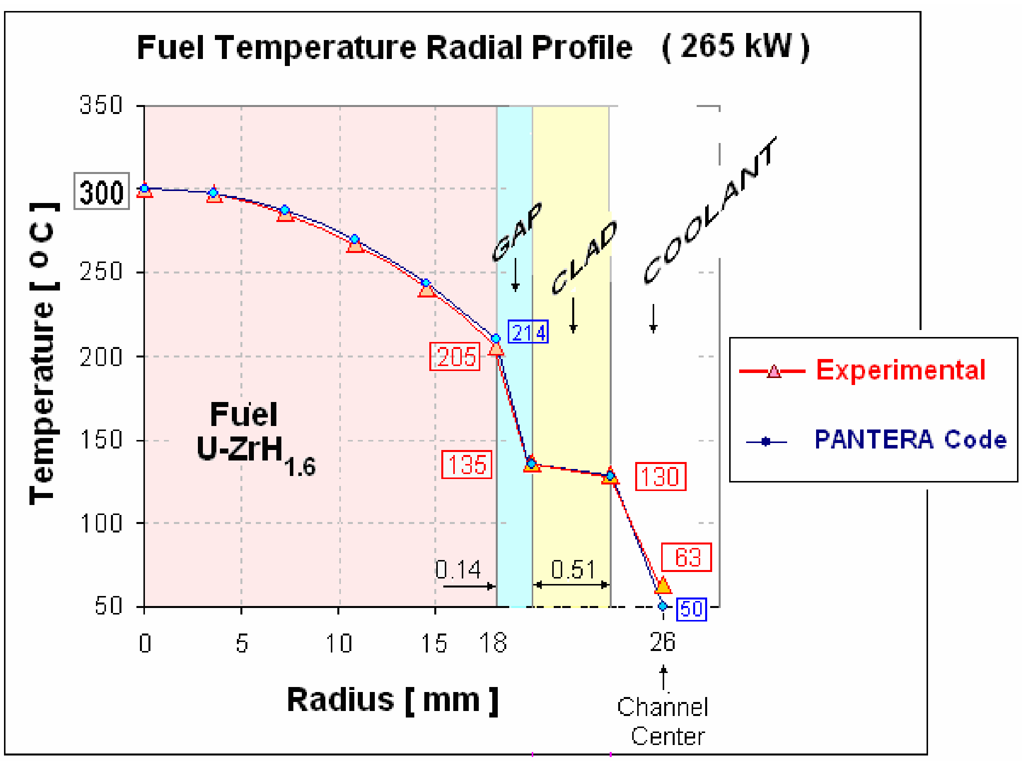

Figure 9. Experimental results of radial temperature profile for the fuel rod in position B1 at 265 kW.

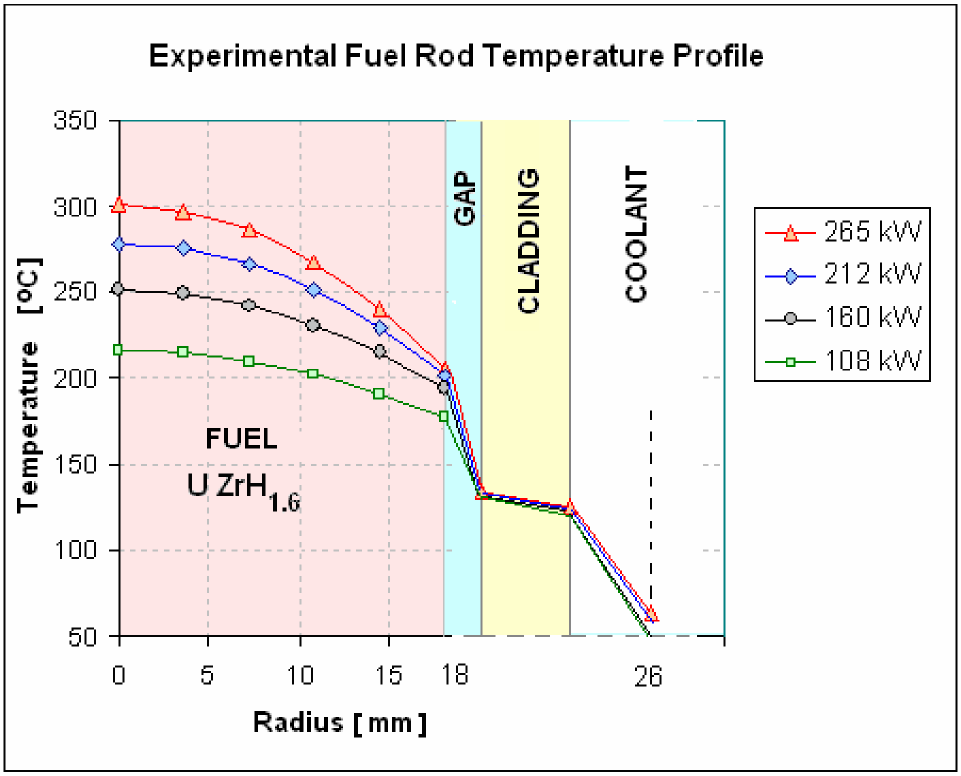

Figure 10. Experimental fuel rod radial temperature profile in position B1 at another reactor powers.

Table 4. Fuel rod temperature profile in the position B1.

Reactor Power [kW]	Temperatures				
	Fuel Center [^{o}C]	Fuel Surface [^{o}C]	Clad Inner [^{o}C]	Clad Outside [^{o}C]	Channel 1 Center [^{o}C]
265	301	205	135	130	63
212	278	201	134	129	57
160	252	194	132	128	46
108	216	177	129	126	43

6. Conclusion

Subcooled pool boiling occurs at above approximately 60 kW on the cladding surface in the central channels of the IPR-R1 TRIGA core. However, the high heat transfer coefficient due to subcooled boiling causes the cladding temperature be quite uniform along most of the active fuel rod region and do not increase very much with the reactor power. The IPR-R1 TRIGA Reactor normally operates in the range from 100 kW until a maximum of 250 kW. On these power levels the heat transfer regime between the clad surface and the coolant is subcooled nucleate boiling. Boiling heat transfer is usually the most efficient heat transfer pattern in nuclear reactors core (Duderstadt and Hamilton, 1998). Another important aspect of the reactor operation safety is that it is far from the occurrence of the departure of nucleate boiling and critical heat flux (Rezende and Mesquita, 2006).

7. Acknowledgments

The authors thank the operation staff of the IPR-R1 TRIGA Reactor for their help during the experiments.

8. References

Ahad, A.O.M.A.; Ahmed, K.; Ahmed, K.F., 1992, "Final Safety Analysis Reporter for the 3MW TRIGA Mark II Research Reactor at AERE". Savar, Dhaka, Bangladesh.

ASME, 1992, "ASME Boiler and Pressure Vessel Code, Section II – Materials, Part D, Properties", The American Society of Mechanical Engineers, New York.

Dalle H.M., 1999, "Neutronic Calculations of the IPR-R1 TRIGA Reactor with WIMSD4 e CITATION". M. Sc dissertation, Universidade Federal de Minas Gerais, Belo Horizonte, (in Portuguese), 183 p.

Dalle H.M., 2003, "Neutronic Analyses of the IPR-R1 TRIGA Reactor with 63 Fuel Elements Configuration and Regulating Control Rod in Position F16", CDTN/CNEN, NI–EC3-01/03, Belo Horizonte, (in Portuguese), 23 p.

Duderstadt J.J and Hamilton L.J., 1976, "Nuclear Reactor Analysis", John Wiley & Sons, Inc. New York, 650 p.

General Atomic,1969, "Safeguards Analysis Report". (GA-9867). San Diego, CA.

General Atomic, 1970, "Safeguards Summary Report for the New York University TRIGA Mark I Reactor". (GA-9864). San Diego. 172 p.

Glasstone S. and Sesonske A., 1994, "Nuclear Reactor Engineering", 4 ed., Chapman and Hall, New York, NY.

Kreith F. and Bohn M. S., 2001, "Principles of Heat Transfer", 6th ed., Brooks/Cole, New York, 805 p.

Gulf General Atomic, 1972, 15" SST Fuel Element Assembly Instrumented Core. San Diego, CA.. Drawing Number TOS210J220.

Lamarsh J.R. and Baratta A.J., 2001, "Introduction to Nuclear Engineering", 3° ed., Upper Saddler River: Prendice Hall, 783 p.

Mesquita A. Z., 2005, "Experimental Investigation on Temperatures Distributions in a Research Nuclear Reactor TRIGA IPR-R1", Ph.D thesis, Universidade Estadual de Campinas, São Paulo, (in Portuguese), 190 p.

Rezende, H.C. and Mesquita, A.Z., 2006, "Experimental Prediction of Departure From Nucleate Boiling on the IPR-R1". Proceedings of the 11th Brazilian Congress of Thermal Sciences and Engineering -- ENCIT 2006, Braz. Soc. of Mechanical Sciences and Engineering - ABCM, Curitiba, Brazil,- Dec. 5-8.

Simnad M.T., Foushee F.C. and West G.B., 1976, "Fuel Elements for Pulsed TRIGA Research Reactors", Nuclear Technology, 28:31-56.

Todreas N.E. and Kazimi M.S., 1990, "Nuclear Systems I: Thermal Hydraulic Fundaments", Hemisphere Publishing Corporation, New York, 705 p.

Tong L. S. and Tang Y.S, 1997, "Boiling Heat Transfer and Two-Phase Flow", 2nd. Ed. Taylor & Francis, Washington.

Tong L.S. and Weisman J., 1996, "Thermal Analysis of Pressurized Water Reactors", Third Edition, American Nuclear Society. Illinois, 748 p.

Veloso M.A., 2005, "Thermal–hydraulic Analyses of the IPR-R1 TRIGA Reactor on 250 kW", CDTN/CNEN, NI-EC3-05/05, Belo Horizonte, (in Portuguese), 166 p.

Wagner W. and Kruse A., 1998, "Properties of Water and Steam – The Industrial Standard IAPWS-IF97 for the Thermodynamics Properties", Springer, Berlin, 354 p.

9. Copyright Notice